

X-ray Microbeam Investigation of Deformation Microstructure under Spherical Indentation in Cu

W. Yang,¹ B.C. Larson,¹ J.Z. Tischler,¹ G.M. Pharr,^{2,1} G.E. Ice, W. Liu,¹ J.D. Budai¹

¹Oak Ridge National Laboratory (ORNL), Oak Ridge, TN, U.S.A.

²University of Tennessee, Knoxville, TN, U.S.A.

Introduction

Indentation has long been a very useful method for characterizing materials and evaluating basic properties of materials [1, 2]. However, classical plasticity theory fails to predict experimentally observed size-effects in microhardness tests that use nanoindentation [3, 4]. This raises a challenge to computational modeling and simulations. Under plastic deformation, dislocations in face-centered materials tend to self-arrange to the patterning structure of geometrically necessary dislocations (GNDs) and statistically stored dislocations (SSDs) [5]. Until recently, nondestructive 3-D microstructural probes that have the submicron, intragranular spatial resolution required to investigate the heterogeneous deformation induced below nanoindents have not been available. By combining submicron-diameter x-ray microbeams with differential-aperture x-ray microscopy (DAXM) depth profiling [6], it is now possible to obtain local orientation and residual stress from submicron voxels (volume elements) of material, thus providing a powerful tool for the nondestructive study of the local microstructure of plastic deformation. In this report, we demonstrate the use of DAXM to investigate (nondestructively) the deformation microstructure under a spherical indent in copper.

Methods and Materials

The experimental microbeam diffraction geometry used at the UNI-CAT beamline at the APS uses Kirkpatrick-Baez mirrors to focus polychromatic synchrotron x-rays to $\sim 0.5 \mu\text{m}$ diameter. A charge-coupled (CCD) area detector is used to collect Laue diffraction images, and a 50- μm -diameter Pt wire is used as a knife-edge absorption profiler to depth-resolve Bragg-diffracted intensity from the sample, as described previously [6]. A dislocation-free Cu single crystal with a $\langle 111 \rangle$ plane normal was subjected to a 200-mN maximum load indent by using a 69- μm -radius spherical tip. The measurement geometry and the crystallographic orientation of the sample and incident microbeam are displayed in the schematic drawing of the scattering geometry and optical micrograph of the indent in Fig. 1. For performing the x-ray microbeam measurements, the surface of the sample was oriented at an angle of 45° with respect to the incident beam so that the microbeam penetrated ~ 30 to $50 \mu\text{m}$ below the surface, limited by beam attenuation for the ~ 8 -22-keV energy range of the polychromatic microbeam.

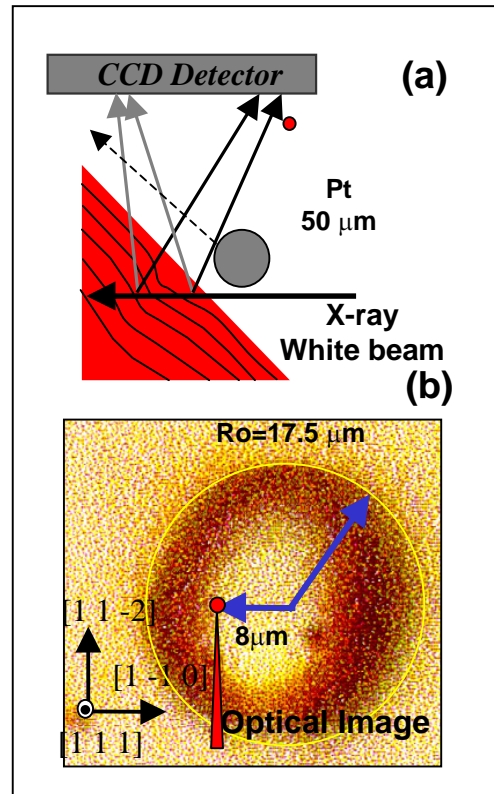


FIG. 1. (a) Diffraction geometry with depth profiler. (b) Optical micrograph of spherical indent in Cu; the red arrow indicates microbeam direction and entry point.

Measurements have been made of plastic strain in the deformed region below pyramidal, conical, and spherical indents. The measurements discussed here were made with the microbeam entering to the left of the center of the spherical indent, as shown in Fig. 1(b). After entering the sample, the beam penetrates through the deformation pattern at a 45° angle [Fig. 1(a)] with respect to the surface and provides full Laue diffraction patterns for each increment along the beam. By depth-resolving these Laue diffraction patterns by using the Pt wire depth profiler [6, 7, 8], micron-by-micron, depth-resolved measurements were made of the 3-D orientation at each position along the beam. Thus the ability to determine plastic strain with 3-D micron resolution was demonstrated and direct information on the nature of the

deformation pattern generated by the 200-mN indentation was provided.

Results and Discussion

Figure 2 is a composite picture containing (a) an enlarged image of the (hhh) reflection, (b) a white microbeam Laue diffraction pattern, (c) a depth-dependent (111) pole figure, and (d) a log-scale graph of the micron-by-micron lattice rotations and rotation axes as a function of depth along the microbeam after it enters the sample at the position shown in Fig. 1(b). Since white Laue patterns represent a one-to-one mapping of local lattice plane orientations in the sample onto the CCD area detector, depth-resolving and analyzing these diffraction patterns provides a direct measure of the indent-induced lattice rotations as a function of depth.

The enlarged image of the (hhh) Laue diffraction pattern in Fig. 2(a) shows clearly that there are significant lattice rotations under the indent (this pattern would be a single spot with no streaking if there were no deformation). The uneven intensity distribution of the streaked pattern indicates qualitatively that a heterogeneous distribution of lattice rotations occurs as a

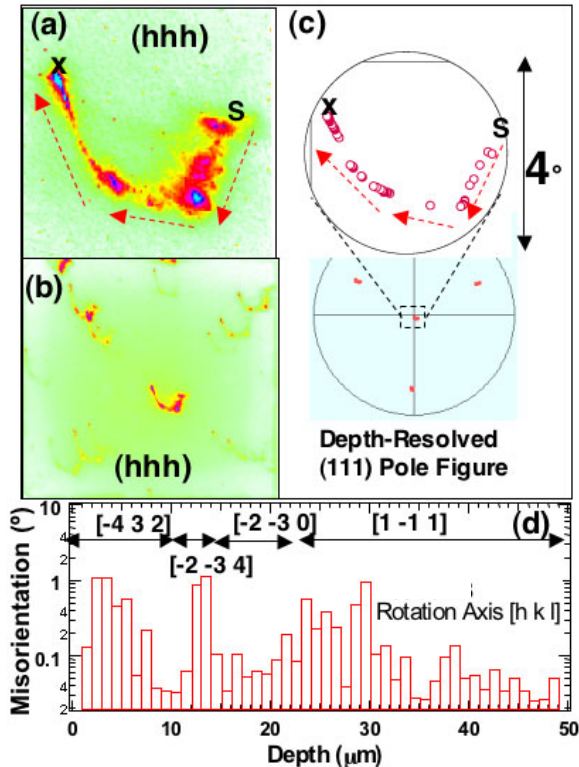


FIG. 2. (a) Enlarged (hhh) Laue pattern. (b) Full microbeam Laue pattern for the measured sample position. (c) Depth-resolved (111) pole figure. (d) Log plot of local misorientation angles as a function of penetration depth, with (approximate) rotation axes grouped around the $[-4\ 3\ 2]$, $[-2\ -3\ 4]$, $[0\ -2\ 1]$ and $[1\ -1\ 1]$ directions.

function of depth along the microbeam. The enlarged pole figure in Fig. 2(c) provides a quantitative, depth-resolved representation of the angular orientations as a function of depth, where each open circle is the result of the analysis of a full Laue diffraction pattern for that depth. The “s” marks and the “x” marks in Figs. 2(a) and 2(c) indicate the surface deformation orientation and the undeformed orientations, respectively. The local misorientation angle (i.e., local orientation at one point compared to the orientation of the following micron) as a function of depth is plotted in Figure 2(d). The rotation axes were found to be grouped (roughly) along three nominal directions — $[-4\ 3\ 2]$, $[-2\ -3\ 4]$, and $[1\ -1\ 1]$ — for this position and penetration direction of the microbeam.

In the absence of crystal lattice effects and dislocation patterning (i.e., dislocation wall formation) [5], a continuous bow-shaped pattern would have been expected in Figs. 2(a) and 2(c). The presence of rather straight lines and clustering at several points indicates that significant patterning is present as a function of depth along the beam penetration direction. This is shown quantitatively in Fig. 2(d), where both the magnitude of the micron-by-micron misorientations and the rotation axes are indicated.

This example of 3-D, micron-resolution, spatially resolved measurements of plastic deformation under a spherical indent illustrates directly that deformation microstructures below indents in face centered metals are complex and that they can be investigated nondestructively and in detail by using the DAXM technique. These spatially resolved measurements along a single line under an indent are not sufficient for a detailed comparison with finite element modeling, multi-scale modeling, or discrete dislocation calculations of nanoindent deformation. However, the presence of discontinuous rotations as a function of depth observed below the smooth spherical indent is in qualitative disagreement with isotropic plasticity considerations, which would predict smoothly varying rotations and rotation axes. X-ray microbeam measurements performed by using this technique to investigate pyramidal and conical indents have shown similar patterning and indent shape effects [7, 8]. Measurements are in progress to investigate the entire deformation volume below indents in order to make detailed comparisons with finite-element and multiscale dislocation modeling calculations.

Acknowledgments

This research was supported by the U.S. Department of Energy (DOE), Office of Science, Office of Basic Energy Sciences (BES), Division of Materials Sciences, under contract with ORNL, managed by UT-Battelle, LLC. UNI-CAT is supported by DOE under Award No. DEFG02-91ER45439 through the Frederick Seitz Materials Research Laboratory at the University of Illinois at Urbana-Champaign; ORNL (DOE Contract No. DE-AC05-00OR22725 with UT-Battelle LLC),

National Institute of Standards and Technology (U.S. Department of Commerce); and UOP LLC. Use of the APS is supported by DOE BES under Contract No W-31-109-ENG-38.

References

- [1] J.B. Thompson, J.H Kindt, B. Drake, H.G. Hansma, D.E. Morse, and P.K. Hansma, *Nature* **414**, 773 (2001).
- [2] B.R. Lawn, N.P. Padture, H.D. Cai, and F. Guiberteau, *Science* **263**, 1114 (1994).
- [3] J.G. Swadener, E.P. George, and G.M. Pharr, *J. Mech. Phys. Solids* **50**, 681 (2002).
- [4] Z. Xue, Y. Huang, K.C. Hwang, and M. Li, *J. Eng. Mater. – Trans. ASME* **124**, 371 (2002).
- [5] D.A. Hughes, N. Hansen, and D.J. Bammann, *Scripta Mater.* **48**, 147 (2003).

[6] B.C. Larson, W. Yang, G.E. Ice, J.D. Budai, and J.Z. Tischler, *Nature* **415**, 887 (2002).

[7] W. Yang, B.C. Larson, G.M. Pharr, G.E. Ice, and J.Z. Tischler, in *Multiscale Phenomena in Materials — Experiments and Modeling Related to Mechanical Behavior*, edited by K.J. Hemker et al. (Materials Research Society, Warrendale, PA, 2003), **779**, W5.3.4.1.

[8] W. Yang, B.C. Larson, G.M. Pharr, G.E. Ice, J.G. Swadener, J.D. Budai, J.Z. Tischler, and W. Liu, *Surface Engineering 2002-Synthesis, Characterization, and Applications*, edited by A. Kumar, W.J. Meng, Y.T. Cheng, J. Zabinski, G.L. Doll, and S. Veprek (Materials Research Society, Warrendale, PA, 2003), **750**, Y8.26.1.